

Improved Cycle Performance of Sulfur-Doped LiFePO₄ Material at High Temperatures

Seung-Byung Lee, Seung-Hyun Cho, Vanchiappan Aravindan, Hyun-Soo Kim, and Yun-Sung Lee*

Faculty of Applied Chemical Engineering, Center for Functional Nano Fine Chemicals, Chonnam National University, Gwangju 500-757, Korea. *E-mail: leeys@chonnam.ac.kr

[†]Battery & Piezoelectric Research Center, Korea Electrotechnology Research Institute, Changwon 641-120, Korea
Received July 22, 2009, Accepted August 8, 2009

Pristine and sulfur-doped (LiFePO_{3.98}S_{0.03}) lithium iron phosphates were synthesized by a sol-gel method. The XRD pattern of the prepared materials suggested an orthorhombic structure with a *Pnma* space group and an absence of impurities. The Li/LiFePO₄ or LiFePO_{3.98}S_{0.03} cells were employed for cycling studies at various temperatures (25, 50 and 60 °C). In all cases, the Li/LiFePO_{3.98}S_{0.03} cell showed an improved performance with a stable discharge behavior of ~155 mAhg⁻¹. Nevertheless, pristine LiFePO₄ cells presented poor discharge behavior at elevated temperatures, especially 60 °C.

Key Words: LiFePO₄, Sulfur ion doping, Cathode material, Sol-gel, High temperature

Introduction

Since its discovery by Padhi *et al.*¹ in 1997, LiFePO₄ has been attractive to researchers as a potential cathode material for lithium batteries given its cost effectiveness, safety, and environmental aspects when compared with commercially employed toxic LiCoO₂. Moreover, its electrochemical profile is very flat, located near 3.45 V *versus* Li/Li⁺, with a relatively high theoretical capacity of 170 mAhg⁻¹ when compared with other proposed alternate candidates for LiCoO₂. Further, the PO₄³⁻ polyanion renders the structure during the lithiation/delithiation process and tunes the Fe^{3+/2+} redox couple to a useful level through an inductive effect. The aforementioned properties have extended the utilization of LiFePO₄ into large-sized power packs related to electric vehicles (EV), hybrid electric vehicles (HEV), and stationary storage batteries. However, the inherent electrical conductivity of LiFePO₄ offers a poor rate capability of the cell, which hinders its real time application. This inborn electronic conductivity has been circumvented by several approaches, including surface coating with carbon²⁻⁷ and doping with metal ions.^{8,9} Synthetic routes were also important factors to determine the electrochemical properties of the material, among the approaches noteworthy for mass production are solid-state,^{10,11} precipitation,¹² and sol-gel¹³⁻¹⁵ methods.

The sol-gel route is a useful technique to achieve single phase and homogeneous particle morphologies with high surface area, which is one of the prerequisites to improve electrochemical performance of the cell. Using this technique, we have succeeded in preparing single-phase LiFePO₄ particles with desired properties.¹⁶ In addition to elevated temperature performance of the cell, EV and HEV applications require high rates. In order to accomplish such applications, an anionic substitution is attractive and appealing. Recently, the F doping into PO₄ sites reported by Liao *et al.*¹⁷ revealed the improved performance of Li/LiFePO₄ cells at elevated temperatures. Sun *et al.*¹⁸ also had reported that substitution of S atoms for O sites in the LiMn₂O₄ lattice provides excellent rate capability

of the cell, even at elevated temperatures.

Reported in this paper for the first time is the synthesis of LiFePO₄ and sulfur-doped LiFePO₄ materials through a conventional sol-gel method without any further treatments, such as carbon coating or ball milling, under optimized conditions. The elevated temperature performance of the cells *viz.* 50 and 60 °C, along with room temperature, were studied and described.

Experimental

LiFePO₄ and sulfur-doped LiFePO₄ materials were synthesized from the starting materials of LiCH₃COO (Sigma-Aldrich, USA), Fe(CH₃COO)₂ (Sigma-Aldrich, USA), H₃PO₄ (Sigma-Aldrich, USA), Li₂S (Sigma-Aldrich, USA), and C₆H₁₀O₄ (Sigma-Aldrich, USA), using a sol-gel method. First, the stoichiometric ratios of each material were dissolved in ethanol and mixed well with an appropriate amount of chelating agent (adipic acid). The solution was evaporated at 90 °C for 4 h to form a transparent gel. The gel was then transferred to a vacuum oven and dried to yield the gel precursors. The resultant precursor was fine ground and calcined at 400 °C for 1.5 h and again heat treated at 670 °C for 2.5 h under an Ar flow using a tubular furnace to yield the LiFePO₄ material. A similar procedure was also conducted to achieve the sulfur-doped LiFePO₄ phase. To determine the content of sulfur, the obtained sulfur-doped LiFePO₄ material was investigated with sulfur analyzer (CS 600, LECO, USA) and the determined composition of sulfur-doped LiFePO₄ was considered as LiFePO_{3.98}S_{0.03}.

Powder X-ray diffraction (XRD, Rint 1000, Rigaku, Japan) studies were performed to analyze the crystalline phase of the synthesized materials under CuK α radiation. Surface morphological features were recorded through a field scanning electron microscope (FE-SEM, S-4700, Hitachi, Japan). Electrochemical characterizations were conducted using a CR2032 coin-type cell. The cathode was fabricated with 20.0 mg of active material, 3.0 mg of Ketzen black, and 3.0 mg of con-

ductive binder such as Teflonized acetylene black (TAB) (2.0 mg of acetylene black and 1.0 mg of graphite). This was then pressed on a 200 mm² stainless steel mesh that was used as the current collector under a pressure of 300 kgcm⁻² and dried at 130 °C for 5 h in an oven. The cell was comprised of a cathode and lithium metal anode separated by a porous polypropylene film (Celgard 3401). The 1.0 M LiPF₆ in ethylene carbonate (EC):dimethyl carbonate (DMC) (1:1 by vol, Techno Semichem, Korea) was chosen as the electrolyte. The current density was fixed at 0.1 mAcm⁻² for cycling studies between the cut-off limits of 2.8 to 4.0 V at various temperatures, viz. 25, 50, and 60 °C.

Results and Discussion

Figure 1 represents the X-ray diffraction patterns of the LiFePO₄ and LiFePO_{3.98}S_{0.03} phases, prepared by the optimized conditions of the conventional sol-gel process under an Ar atmosphere. The two materials exhibited an orthorhombic structure with a *Pnma* space group. The crystalline phases of the materials were indexed according to the JCPDS card No. 40-1499. Both LiFePO₄ and LiFePO_{3.98}S_{0.03} material did not indicate the presence of any impurity phases, such as Li₃PO₄, FeP, and Fe₂P.¹⁹ This confirmed the excellent phase purity of the prepared olivine phase. The lattice constants of the LiFePO_{3.98}S_{0.03} material were: *a* = 10.3127 Å; *b* = 6.0043 Å; *c* = 4.6899 Å, similar to those of the LiFePO₄ material (*a* = 10.3228 Å, *b* = 6.0049 Å, *c* = 4.6913 Å).¹⁶ There was a small decrease in the *a*-axis parameter, however, there was no remarkable change in the lattice constants in the other axes. The anionic substitution of sulfur did not alter the crystalline nature of the host lattice.

Figure 2(a) and 2(b) show the scanning electron microscope (SEM) images of the LiFePO₄ and LiFePO_{3.98}S_{0.03} materials synthesized by the sol-gel method. The LiFePO₄ phase was composed of many poly crystalline type particles within a range of 50 - 100 nm, and large particles between 200 - 300 nm size, all distributed randomly. However, the LiFePO_{3.98}S_{0.03} material bore a composition similar to pristine LiFePO₄,

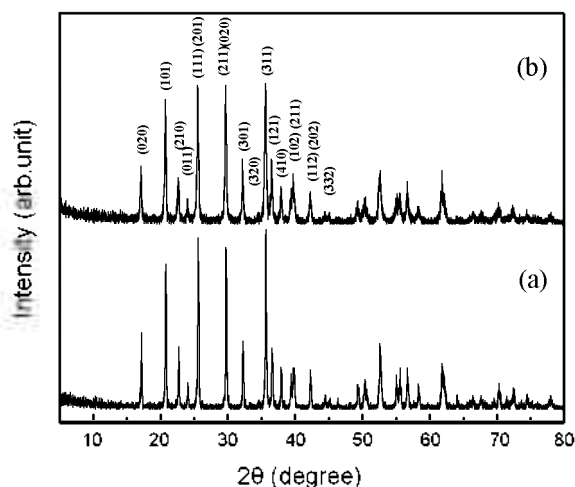


Figure 1. XRD patterns of (a) LiFePO₄ and (b) LiFePO_{3.98}S_{0.03} materials obtained by the sol-gel method.

with small particles between 20 - 50 nm and bigger particles between 250 - 300 nm. The primary particles of the sulfur-doped LiFePO₄ were smaller than that of the LiFePO₄ material, but the secondary particles presented the larger sized particles for the LiFePO_{3.98}S_{0.03}, due possibly to the weak aggregation of such particles after sulfur doping. At lower concentrations of doping, elements were very hard to detect through X-ray diffractograms. In order to confirm the presence of sulfur in the LiFePO_{3.98}S_{0.03} phase, energy dispersive X-ray spectroscopy was performed and is presented in Fig. 2(c). This spectrum was recorded against the X-ray emission of elements present in the specimen as a function of electron volts (eV). The weakly intense peak adjacent to P, near 2.5 - 2.8 keV, confirmed the presence of sulfur in the olivine phase. The weak intensity of the sulfur may be attributed to its composition present in the material as confirmed by sulfur analysis.

Figure 3 also shows the particle distribution of the LiFePO₄ and LiFePO_{3.98}S_{0.03} materials synthesized by the sol-gel method and clearly presents that the majority of the particles lies between 50 - 100 nm for pure LiFePO₄, while the LiFePO_{3.98}S_{0.03} particles are observed between 20 - 50 nm. The drastic reductions in particle sizes are attributed to the inclusion of the sulfur ion in the LiFePO₄ structure during the synthetic process. It was concluded that the sulfur doping can effectively control

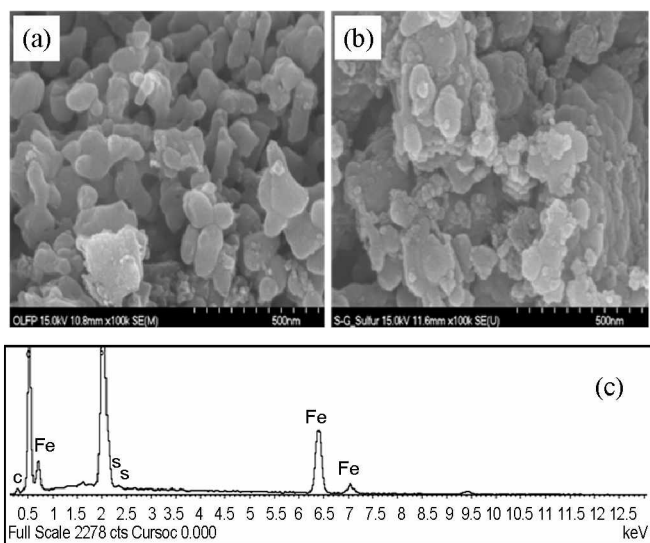


Figure 2. SEM images of: (a) LiFePO₄; (b) LiFePO_{3.98}S_{0.03}; (c) EDX traces of LiFePO_{3.98}S_{0.03} by the sol-gel method.

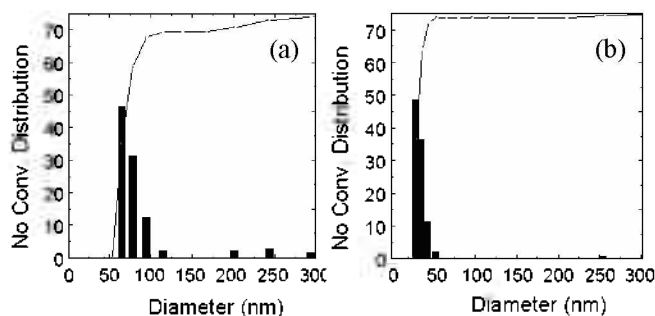


Figure 3. Particle size distribution of: (a) LiFePO₄; (b) LiFePO_{3.98}S_{0.03} by the sol-gel method.

the particle size of the LiFePO_4 material and its large secondary particles, due to weak aggregation, will help stabilize the $\text{Li}/\text{LiFePO}_4$ cell during the electrochemical test.

Figure 4 presents the results of the electrochemical characterization of the $\text{Li}/\text{LiFePO}_4$ and $\text{Li}/\text{LiFePO}_{3.98}\text{S}_{0.03}$ cells between 4.0 and 2.8 V, using a constant current density of 0.1 mAcm^{-2} at ambient temperature. A well-defined, long distinct plateau at $\sim 3.4 \text{ V}$ corresponds to the phase purity of the prepared material. The cells showed initial discharge capacities of 149 and 154 mAhg^{-1} for the LiFePO_4 and $\text{LiFePO}_{3.98}\text{S}_{0.03}$ phases. At a second cycle, the discharge capacities were slightly increased to 152 and 155 mAhg^{-1} , respectively. It is noticeable that, after the second cycle, both cells almost delivered stable discharge behavior for the observed 30 cycles. This also confirms the excellent reversibility of the materials prepared, in addition to high capacity and good cycle retention. It is well known that the wet synthesis process can produce a homogeneous powder owing to its small particle size, strong interactions between metal ions brought about by chelation, and a long mixing time in aqueous solution.¹⁶ Therefore, the resulting material obtained by the sol-gel route can provide superior electrochemical performance. Park *et al.*²⁰ also had reported that sulfur doping in LiNiO_2 material greatly improves the stability of the LiNiO_2 structure during charge/discharge process. They suggested that partial substitution of oxygen with sulfur for LiNiO_2 might create a more flexible structure the electronegativity of sulfur is lower than that of oxygen, which prevents the disintegration of the structure by the elongation of lithium ions during cycling. We speculate that sulfur doping in LiFePO_4 material also could be produced small structural change in LiFePO_4 powder, which can produce a good effect to the increase of ion transport for lithium by the sulfur

doping, except merit of the easy synthesis of LiFePO_4 with very small primary particle. A more detailed electrochemical and structural discussion regarding the role of the sulfur ion in the LiFePO_4 material, will be reported elsewhere. Meanwhile, Xu *et al.*²¹ demonstrated the synthesis of LiFePO_4 by a poly (ethylene glycol)-assisted sol-gel route and achieved good discharge capacity. The material exhibited a discharge capacity ($\sim 160 \text{ mAhg}^{-1}$) very close to its theoretical value of 170 mAhg^{-1} , revealing a good rate capability and stable cycle life.²⁰ Nevertheless, there is no report for high temperature performance of the cell.

In this context, adipic acid-mediated synthesis of LiFePO_4 and $\text{LiFePO}_{3.98}\text{S}_{0.03}$ are subjected to elevated temperature studies (50 and 60°C) as shown in Fig. 4. At 50°C , the cells experienced initial discharge capacities of 150 and 153 mAhg^{-1} for LiFePO_4 and $\text{LiFePO}_{3.98}\text{S}_{0.03}$, respectively. Increasing capacity trends were observed for both cells in the first few cycles, beyond that, those cells delivered stable behavior with negligible amounts of capacity variations. The cells presented the capacity of 152 and 156 mAhg^{-1} for LiFePO_4 and $\text{LiFePO}_{3.98}\text{S}_{0.03}$ after stabilization. On the other hand, different capacity profiles were observed at 60°C for the pure olivine phase. The first discharge capacity of 148 and 155 mAhg^{-1} were obtained for the LiFePO_4 and $\text{LiFePO}_{3.98}\text{S}_{0.03}$ materials. The $\text{Li}/\text{LiFePO}_{3.98}\text{S}_{0.03}$ cell showed near stable behavior similar to those at 25 and 50°C , with a $> 99.9\%$ capacity retention compared to the first cycle. However, the pure LiFePO_4 experienced a continuous capacity fading as well as reduced initial discharge capacity at this temperature (60°C). The excellent cycling performance of the sulfur-doped LiFePO_4 may be attributed to substitution of larger ion radii containing elements that may generate a channel with

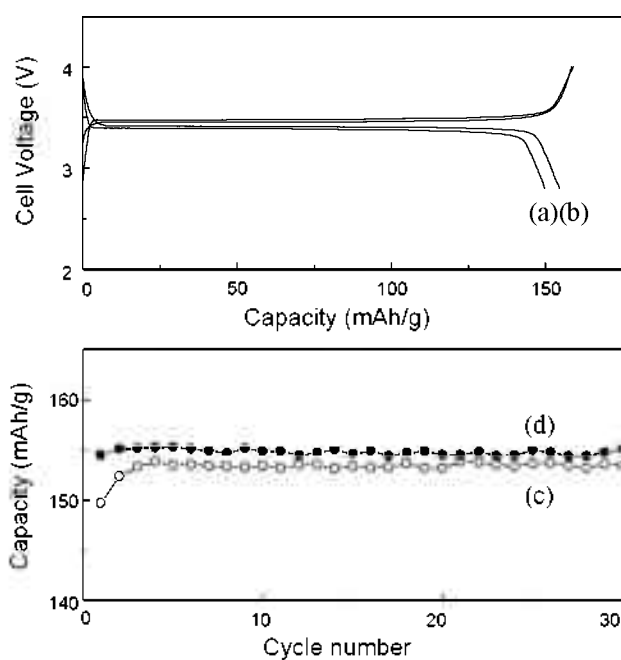


Figure 4. First charge/discharge curves of: (a) LiFePO_4 ; (b) $\text{LiFePO}_{3.98}\text{S}_{0.03}$, and cycle performance of: (c) LiFePO_4 ; (d) $\text{LiFePO}_{3.98}\text{S}_{0.03}$ materials at room temperature.

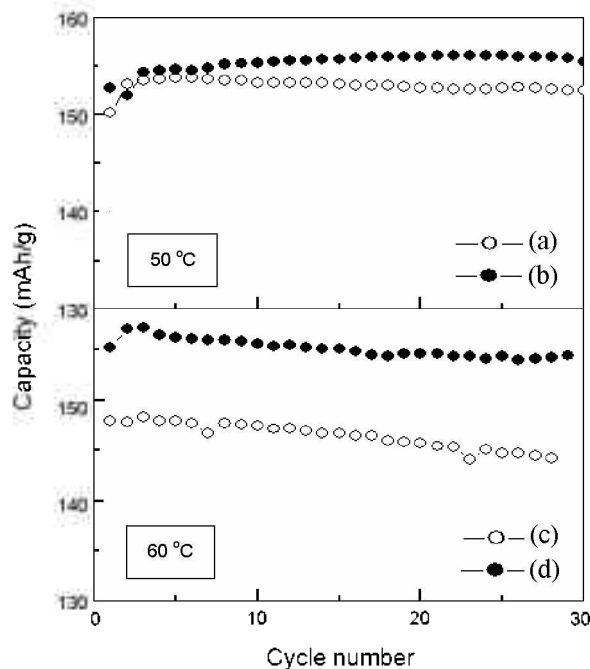


Figure 5. Cycle performances of: (a) LiFePO_4 ; (b) $\text{LiFePO}_{3.98}\text{S}_{0.03}$ at 50°C ; and (c) LiFePO_4 ; (d) $\text{LiFePO}_{3.98}\text{S}_{0.03}$ at 60°C .

faster mobility of the Li^+ ions during the cycling process.²² In addition, the ionic radius of S^{2-} was 0.184 nm, larger than O^{2-} (0.14 nm).²³ Further, both elements showed good replacement mechanisms by way of the other. Meanwhile, it was reported that dopants with larger ion radii may stabilize the structure.²⁴ This is in good agreement with the study herein, especially at higher temperatures. The poor performance of LiFePO_4 at high temperature may be ascribed to the electrochemical reaction involving LiFePO_4 in a LiPF_6 -based non-aqueous electrolyte. When charging, oxidation of the electrolyte, besides HF content present in the electrolyte, generates H^+ at the electrode surface (solid electrolyte interface), with the H^+ ions exchanging for Li^+ within the electrode. Now, both lithium ions and protons exist within the olivine framework of the electrode²⁴ and it has been shown that EC and DMC may be oxidized at the potentials used here. Oxidation of such electrolyte solvents originates at the carbonyl group and can lead to eviction of H^+ .²⁵⁻²⁷ The cyclic carbonates (EC) are more reactive than their linear counterparts (DMC). The oxidation of such electrolyte solutions can also provide electrons in the external circuit. Regarding the discharging process, electrochemical reduction within the electrolyte consumes protons, thus driving its extraction from the electrode and its replacement by Li^+ .²⁵⁻²⁷ In the case of sulfur-doped LiFePO_4 , the presence of sulfur in the olivine host hinders such adverse reactions with electrolyte solutions to provide excellent electrochemical properties at elevated temperatures.

Conclusions

Pristine LiFePO_4 and sulfur-doped ($\text{LiFePO}_{3.98}\text{S}_{0.03}$) materials were synthesized by a sol-gel route under optimized conditions. Both materials exhibited well developed and phase pure structural properties. The $\text{LiFePO}_{3.98}\text{S}_{0.03}$ material, composed of small polycrystalline particles (10 - 50 nm) distributed along with the larger particles, was observed through SEM. The $\text{LiFePO}_{3.98}\text{S}_{0.03}$ cell showed nearly identical discharge capacities ($\sim 155 \text{ mAhg}^{-1}$) for all temperatures studied with stable behavior due to the substitution of O^{2-} with S^{2-} . It is thus the conclusion of the authors that sulfur doping in the LiFePO_4 material can be a key parameter to improve cell performance of the Li/LiFePO_4 at high temperatures.

Acknowledgments. This research was supported by a grant (code #: 2009K000446) from the 'Center for Nanostructured Materials Technology' under the '21st Century Frontier R&D Programs' of the Ministry of Education, Science and Technology, Korea.

References

1. Padhi, A. K.; Nanjundaswamy, K. S.; Goodenough, J. B. *J. Electrochem. Soc.* **1997**, *144*, 1188.
2. Huang, H.; Yin, S. C.; Nazar, L. F. *Electrochem. Solid-State Lett.* **2001**, *4*, A170.
3. Yang, S.; Song, Y.; Zavalij, P. Y.; Whittingham, M. S. *Electrochem. Commun.* **2002**, *4*, 239.
4. Croce, F.; Epifanio, A. D.; Hassou, J. *Electrochem. Solid-State Lett.* **2002**, *5*, A47.
5. Dominko, R.; Goupil, J. M.; Bele, M. *J. Electrochem. Soc.* **2005**, *152*, A843.
6. Spong, A. D.; Vitins, G.; Owen, J. R. *J. Electrochem. Soc.* **2005**, *152*, A2376.
7. Sides, C. R.; Croce, F.; Young, V. Y. *Electrochem. Solid-State Lett.* **2005**, *8*, A484.
8. Chung, S. Y.; Bloking, J. T.; Chiang, Y. M. *Nat. Mater.* **2002**, *1*, 123.
9. Wang, G. X.; Bewlay, S.; Yad, J. *Electrochem. Solid-State Lett.* **2002**, *7*, A503.
10. Andersson, A. S.; Kalska, B.; Thomas, J. O. *Solid State Ionics* **2000**, *130*, 41.
11. Andersson, A. S.; Thomas, J. O. *J. Power Sources* **2001**, 97-98, 508.
12. Delacourt, C.; Poizot, P.; Levasseur, S. *Electrochem. Solid-State Lett.* **2006**, *9*, A352.
13. Yang, J. S.; Xu, J. J. *J. Electrochem. Soc.* **2006**, *153*, A716.
14. Sanchez, M. A.; Brito, G. E.; Fantini, M. C. *Solid State Ionics* **2006**, *177*, 497.
15. Guo, Z. P.; Liu, H.; Bewlay, S. *J. New Mater. Electrochem. Syst.* **2003**, *6*, 259.
16. Lee, S. B.; Cho, S. H.; Cho, S. J.; Park, G. J.; Park, S. H.; Lee, Y. S. *Electrochem. Commun.* **2008**, *10*, 1219.
17. Liao, X. Z.; He, Y. S.; Ma, Z. F. *J. Power Sources* **2007**, *174*, 720.
18. Sun, Y. K.; Oh, S. W.; Yoon, C. S.; Bang, H. J.; Prakash, J. J. *J. Power Sources* **2006**, *161*, 19.
19. Rho, Y. H.; Nazar, L. F.; Perry, L.; Ryan, D. *J. Electrochem. Soc.* **2007**, *154*, A283.
20. Park, S. H.; Sun, Y. K.; Park, K. S.; Nahm, K. S.; Lee, Y. S.; Yoshio, M. *Electrochimica Acta* **2002**, *47*, 1721.
21. Xu, Z.; Xu, L.; Lai, Q. *Mater. Res. Bull.* **2007**, *42*, 883.
22. Su, Z.; Lu, Z. W.; Gao, X. P.; Shen, P. W.; Liu, X. J.; Wang, J. Q. *J. Power Sources* **2009**, *189*, 411.
23. http://en.wikipedia.org/wiki/Ionic_radius
24. Myung, S. T.; Komaba, S.; Kumagai, N. *J. Electrochem. Soc.* **2002**, *149*, A1349.
25. Kolytyn, M.; Aurbach, D.; Nazar, L.; Ellis, B. *J. Power Sources* **2007**, *174*, 1241.
26. Kolytyn, M.; Aurbach, D.; Nazar, L.; Ellis, B. *Electrochem. Solid-State Lett.* **2007**, *10*, A40.
27. Moshkovich, M.; Cojocaru, M.; Gottlieb, H. E.; Aurbach, D. *J. Electroanal. Chem.* **2001**, *497*, 84.